Publishing House
A K A P I T

APPLICATION OF THE CELLULAR AUTOMATA METHOD TO MODELLING LOWER BAINITE IN STEELS

GRZEGORZ JABŁOŃSKI, BOGDAN PAWŁOWSKI*, MACIEJ PIETRZYK

Akademia Górniczo-Hutnicza, al. Mickiewicza 30, 30-059 Kraków, Poland
*Corresponding Author: bpawlow@agh.edu.pl

Abstract

Cellular automata model for bainitic transformation in steels is presented in the paper. Discrete character of the CA method allowed to reproduce formulation of carbides in the bainitic ferrite. Numerical tests have shown that the model predicts qualitatively well physical phenomena occurring during the bainitic transformation. Although the quantitative accuracy concerning morphology of bainite and kinetics of transformation is not satisfactory, the predictive capabilities of the model are much wider comparing to the existing conventional models. It is expected that further research focused on identification of the model parameters should improve the accuracy noticeably.

Key words: cellular automata model, bainitic transformation, lower bainite

1. INTRODUCTION

The tendency to increase strength-to-density ratio, as well as decreasing the production costs, will be probably the main goals of research on materials processing for many years. Steels are competing with other materials in this area and pursuit for new steels, with higher strength, is the objective of research in several laboratories in the world. Advanced high strength steels (AHSS) used by the automotive industry are an example of great progress as far as density-to-strength ratio is considered (Hofmann et al., 2009). As it was shown (Waengler et al., 2008; Morozov et al., 2008; Kuziak et al., 2011b), new generation bainitic steels are another alternative in this area. The bainitic steels, which were widely researched in 50-ies and 60-ies of the last century, see eg. (Honeycombe & Pickering, 1972), were considered as not applicable. Low ductility of these steels limited their practical applications. However, recent research have shown that by decrease of the carbon content and control of the mechanisms of bainite formation, ductility of these steels can be noticeably improved (Kuziak et al., 2011b), while their high strength is maintained. In all these steels bainite plays crucial role in improvement the strength. Kuziak et al. (2011a) presented research on application of bainitic steels to manufacturing of fasteners.

Required volume fraction and morphology of bainite in these steels is obtained by precise controll of cooling process after hot rolling of strips or rods or wire rods, without additional heat treatment. This control of cooling is the main difficulty, which limits introduction of new generation of bainitic steels in the industrial practice. It is expected that computer aided technology design based on modelling should overcome these difficulties. This approach requires realistic and accurate models of the bainitic transformation.

Modelling of bainitic transformation has been for years based on the Avrami type equation. Various improvements were introduced by scientists to

this approach. Recapitulation of these works and advanced model of bainitic transformation can be found in the papers of Bhadeshia and co-workers (Bhadeshia & Edmonds, 1980; Bhadeshia, 2001). Modelling of phase transformation has been developing during thet last two decades. Phase field method, as well as discrete methods Monte Carlo and Cellular Automata, were applied. General idea of the phase field modelling of phase transformation is given by Militzer (2011). This method was originally developed for the solidification process. Even though there are a variety of PFM approaches to solid state transformations available now, a significant body of the simulation work for steels has been conducted for the austenite-ferrite transformation. Capability of prediction of development of the Widmanstätten ferrite is one of the advantages of this method. Monte Carlo method has been applied for improvement of the JMAK approach, see eg. (Abinandanan, 1998; Kooi, 2004).

It seems that lack of capability to predict morphology of bainitic ferrite and hard constituents is the main drawback of the discussed models, which limits their usefulness in design of the new generation steels containing bainite. Thus, the main objective of the present work is search for the alternative modelling technique, which will supply information about structure of the bainitic phase depending on the temperature of transformation and cooling rate. Cellular automata (CA), which is a discrete modelling technique and, therefore, is expected to predict realistically forming of the structure of bainite, was selected in the present work. The first approach to the CA modelling of the bainitic transformation is described in this work.

2. BAINITIC TRANSFORMATION

Phase transformations in steels are divided into two groups: transformation controlled by diffusion and non-diffusive (martensitic) controlled by shear. Bainitic transformation combines features of diffusive and non-diffusive (controlled by slip) transformations (Bhadeshia & Edmonds, 1980). The bainitic ferrite is created by shear mechanism without diffusion. The carbon, which is disposed from the bainitic ferrite, is transported by diffusion into remaining austenite and in the area between the lamellas of the bainitic ferrite.

Classical bainite is defined as micro-composite composed of bainitic ferrite and carbides, resulting from the austenite decomposition. Carbides precipitate in a non-coordinated way together with the ferrite. Lack of coordination causes that in the initial phase of the transformation bainitic ferrite is created and, after that, the remaining austenite becomes richer in carbon and is decomposed into carbides and low temperature transformation products. The morphological types of bainite are discussed by Bhadeshia (2001), Zajac et al. (2005) and Kuziak et al (2011b). In this Chapter key features of bainitic transformation, which are important for modelling, are presented briefly.

2.1. Morphological types of bainite

Originally two morphological types of bainite were distinguished, namely, upper and lower bainite. However, invention of the incomplete austenite transformation resulted in the change in understanding of the mechanisms of bainite formation. The
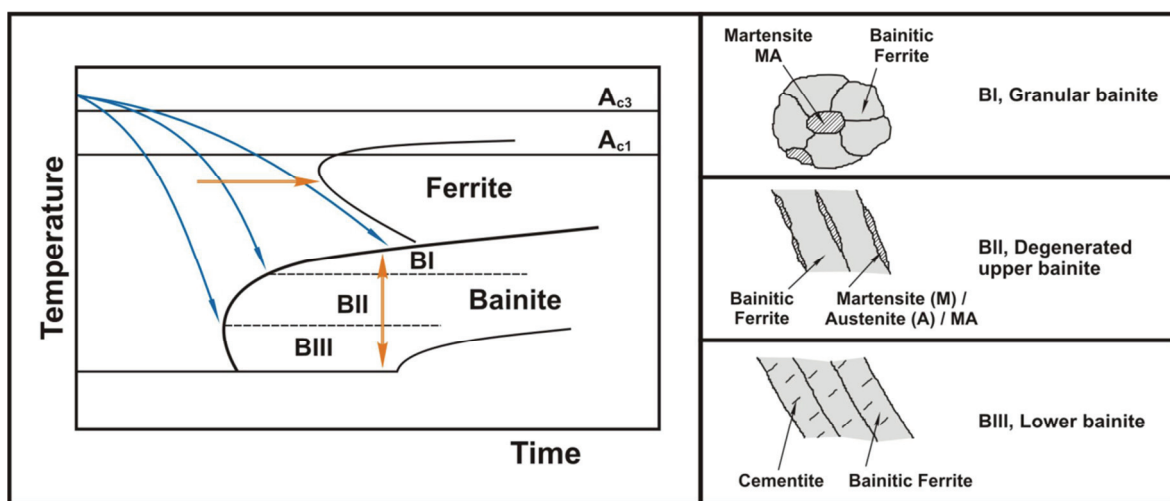
Fig. 1. *Classification and conditions for occurrence of morphological types of the bainite: granular bainite (BI), degenerated upper bainite (BII) and lower bainite (BIII).*

bainite is now defined as microstructure composed of bainitic ferrite and hard phase components with much higher hardness. Figure 1 shows an example of modern classification of morphological types of bainite (Kuziak et al., 2011b).

Beyond the two main types of the bainite (upper and lower), classification in figure 1 distinguishes additionally degenerated upper bainite and granular bainite. In both these types of bainite, the layers or particles composed of austenite and martensite are the hard component of the bainite (MA component). The term degenerated means that the microstructure contains products of incomplete austenite transformation. Zajac et al. (2005) and Morozov et al. (2008) have shown that, depending on the chemical composition and on the conditions of heat treatment, the hard component in bainitic steels can have various morphological forms, which were not considered earlier. Ranges of the temperature, in which various morphological types of the bainite become dominating, are presented in figure 1, as well. More information concerning morphological types of bainite supported by the transmission microscopy pictures can be found in the literature (Bhadeshia, 2001; Kuziak et al., 2011b).

2.2. Modelling bainitic transformation

Characteristic features of the bainitic transformation, which are presented in the previous section, show that modelling of this transformation is difficult. Indeed, the models which predict the kinetics of transformation can be developed, see below and (Kuziak et al., 2011b), where the model based on the Avrami equations with coefficients determined from dilatometric tests using inverse analysis, is described. On the other hand, prediction of the morphology of bainite shown in figure 1 is still a challenge. An attempt to apply Cellular Automata to reach this goal is an objective of this work.

Prediction of the start temperature (B_s) for the bainitic transformation is the first task of modelling. Various equations describing B_s as a function of the steel composition can be found in the scientific literature, see eg. (Bhadeshia, 2001; Kuziak et al., 2011b). The equation proposed by Bhadeshia (2001) is used in the present work:

$$B_s = 637 - 58[C] - 35[Mn] - 15[Ni] - 34[Cr] - 41[Mo] \qquad (1)$$

where symbols of elements represent concentration of these elements in steel in weight percent.

Several researchers proposed the bainitic transformation model composed of nucleation and growth, see for example (Bhadeshia, 2001; Luzginova et al., 2008; Mahnken et al., 2011; Sidhu et al., 2011). Model developed by Bhadeshia (2001) is now considered as the fundamental work on description of the bainitic transformation and this model is presented briefly below. Bhadeshia assumed that nucleation rate I is independent of the steel grade:

$$I \propto \nu \exp\left(\frac{G^*}{R\hat{T}}\right) \Rightarrow$$

$$I = C_3 \exp\left(-\frac{C_4}{RT} - \frac{C_4 \Delta G_m}{C_2 R\hat{T}}\right) \qquad (2)$$

where: G^* - activation energy, which comes from the resistance of the lattice to the motion of dislocations, ν – an attempt frequency, $C_1 = 3.637$ J/(mol·K), $C_2 = 2540$ J/mol, ΔG_m – maximum value of the Gibbs free energy per unit volume of ferrite, $\hat{T}$ – absolute temperature.

In equation (2) C_3 and C_4 are obtained by fitting to the experimental data. C_3 is a product of a number density of nucleation sites and an attempt frequency ν.

Since it depends on the mechanism of the growth, modelling of the growth is rather complicated. The displacement of the interface requires the atoms of the parent phase to be transferred into and adopted by the crystal structure of the product phase. The ease, with which it happens, determines the interface mobility. The velocity of the interface is under mixed control of the diffusion and mobility. Thus, estimation of the volume fraction of bainite requires accounting for nucleation, growth and impingement between grains. The equation describing kinetics of growth of bainite proposed by Bhadeshia (2001) is:

$$X_b = 1 - \exp\left(-\frac{\pi}{3}G^3 I t^4\right) \qquad (3)$$

where: X_b – volume fraction of bainite, G – rate of growth, t – time.

Equation (3) is equivalent to the Avrami equation, which is often used for prediction of the kinetics of the bainitic transformation:

$$X_b = 1 - \exp\left(-kt^n\right) \qquad (4)$$

Although it is not advised (Bhadeshia, 2001), relation of the coefficients k and n on free energy and

nucleation rate is often not accounted for directly and these coefficients are determined using results of dilatometric tests and inverse analysis (eg. Kuziak et al., 2011b). Theoretical considerations show that, according to the type of transformation (nucleation and growth process, site saturation process), a constant value of coefficient n in equation (4) can be used. On contrary, value of the coefficient k must vary with temperature in a way linked to the form of a Time–Temperature–Transformation (TTT) diagram. The formalism of the function $k = f(T)$ must be carefully chosen to describe properly the temperature dependence of k. Thus, a modified Gaussian function is proposed for bainitic transformation by Donay et al. (1996). Simpler exponential relationship is introduced by Kuziak et al. (2011b). Solutions based on Avrami equation were determined for isothermal conditions, therefore Sheil additivity rule (Sheil, 1935) has to be applied for modelling transformation in varying temperatures.

Suehiro et al. (1992) and van Bohemena and Sietsma (2010) proposed the model based on differential equation describing progress of the bainitic transformation. It is more advanced approach, which accounts for the thermodynamic background. This model can be directly applied to phase transformations in varying temperatures.

It is expected that application of the model developed for the ferritic transformation and based on the finite element solution of the diffusion equation in front of the moving interface boundary (Stefan problem) should be effective in modelling bainitic transformation, as well. This solution for the ferritic transformation was performed by Pernach and Pietrzyk (2008). It was possible to predict distribution of the carbon concentration in front of the interface boundary and, further, on the basis of these data to simulate properties of products of austenite decomposition (bainite and martensite), as shown by Pernach and Pietrzyk (2011). Adaptation of this model to simulation of the morphology of bainite would require accounting for the discontinuous process of formation of carbides. It is not trivial and several changes in the FE diffusion model are required.

Recapitulating, analysis of numerous publications shows that kinetics of the increase of the volume fraction of bainite is well described by the Avrami type equation. Good results obtained form such a model for bainitic transformation are shown in earlier Authors publication (Kuziak et al., 2011b). However, prediction of the morphology of the bainite shown in figure 1 requires control of the diffusion

process. It can be done either by the solution of the diffusion equation or by discrete methods. Since the former approach requires long computing times, the latter method is considered in the present work. Among various discrete methods the cellular automata method, which proved its capability in modelling ferritic transformation (Zhang et al., 2003; Lan et al., 2004; Kundu et al., 2004; Opara, 2009; Pietrzyk et al., 2010), was selected. At the first approach the diffusion of carbon is simplified and changes of the carbon concentrations in CA cells is calculated from the equation describing the distance of the diffusion (Christian, 1975).

2.3. Key features of bainitic transformation, which are important for CA modelling

Key features of bainitic transformation, which were the basis of the CA transition rules developed in the present work, are discussed briefly in this section. There are three distinct events in the evolution of bainite (Bhadeshia, 2001). A sub-unit nucleates first at the austenite grain boundary, due to low carbon concentration in this area. The sub-unit lengthens until its growth is arrested by plastic deformation within the austenite. New sub-units then nucleate at its tip and the sheaf structure develops. The number of sheaves growing from different regions determines the volume fraction of the bainite. Carbide precipitation influences the transformation by removing carbon either from the residual austenite or from the supersaturated ferrite. As it can be observed in the schematic TTT diagram in figure 2, transformation is delayed after the temperature below B_s is reached. This delayed time is known as the incubation time. In figure 2 T_{bmax} denotes the temperature corresponding to the shortest incubation time. Figure 2 shows that the bainite growth rate in the TTT-diagrams follows a C-curve.

Two different cases have to be distinguished in modelling bainitic transformation. For upper bainite at high temperature there is carbon diffusion within the austenite followed by carbide precipitation from austenite. For lower bainite at low temperature there is carbon diffusion into austenite and carbide precipitation in ferrite, followed by carbide precipitation from austenite (Mahnken et al., 2011). The primary analysis in the present work is constrained to the lower bainite, in which the carbides occur inside the lamellas of the ferrite. In the CA model this process is controlled by discrete change of the state of the

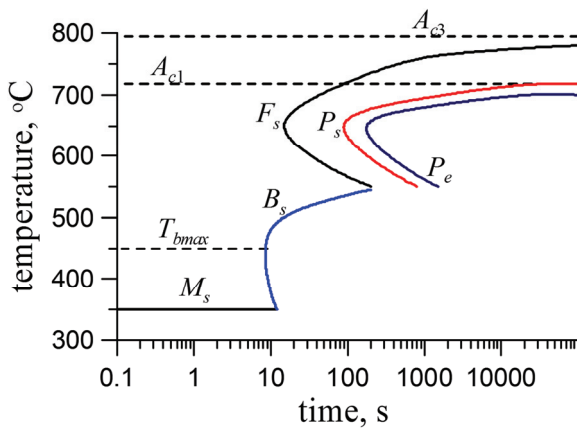cell into carbide when carbon concentration exceeds certain level.

Fig. 2. *Schematic Time–Temperature–Transformation diagram with temperature T_{bmax} corresponding to the shortest incubation time of bainite.*
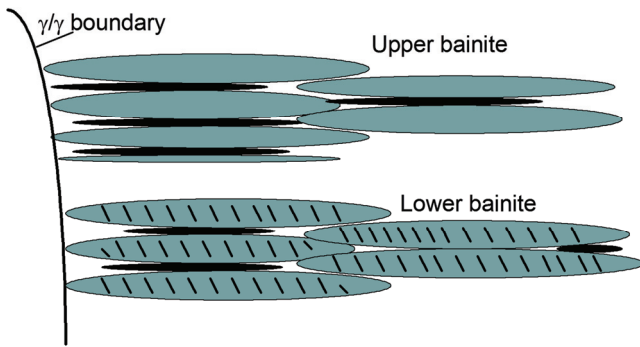

Fig. 3. *Schematic illustration of the sheaves growing in the upper and lower bainite.*

3. CA MODEL

The general idea of modelling of phase transformation presented by Opara (2009) is used in the present work. The states of cells and transition rules relevant for the bainitic transformation are formulated. The computer code developed by Opara (2009) was used to generate the microstructure at the beginning of the bainitic transformation. This microstructure was composed of ferrite and austenite grains.

3.1. General assumptions

The start temperature for the bainitic transformation was calculated from equation (1). The model is general but all results will be presented for the bainitic steel containing 0.07%C, 1.60%Mn, 0.30%Mo, 0.05%V, 0.05%Nb and 0.02%Ti. The equilibrium carbon content in austenite at the austenite-ferrite boundary ($c_{\gamma\alpha}$) and at the austenite-cementite boundary ($c_{\gamma\beta}$) were determined using ThermoCalc software:

$$c_{\gamma\alpha} = -0.004162162T + 3.795891892 \quad (5)$$

$$c_{\gamma\beta} = 0.003182898T - 1.54396674 \quad (6)$$

The equilibrium carbon content in ferrite (c_α) was also determined using ThermoCalc software:

$$c_\alpha = 0.000117838T + 0.1074681 \quad (7)$$

where: T – temperature in ^{o}C.

Simulation of the bainitic transformation is finished when either whole austenite is transformed into bainite or the temperature drops below the martensite start temperature:

$$M_s = 539 - 423[C] - 30.4[Mn] - 7.7[Ni] -$$
$$12.1[Cr] - 7.5[Mo] - 10[Co] \quad (8)$$

The element 0.2×0.2 mm divided into 200×200 cells was considered. Periodic boundary conditions and Moore neighbourhood were applied. The temperature was uniform in the whole element and it was changing according to the assumed external cooling rate. One step of the CA model was equal to 0.1 s.

3.2. States of cells and internal variables

In the CA model states of cells and internal variables have to be defined. The following states of cells are introduced:
α – ferrite,
γ – austenite,
B – bainitic ferrite,
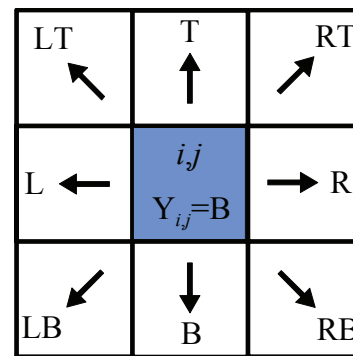χ – carbide.

Fig. 4. *Admissible directions of growth of bainitic ferrite.*

The following internal variables are introduced:
$c_{i,j}$ – carbon concentration in the cell (i,j),
$X_{i,j}$ – volume fraction of the bainitic ferrite in the cell (i,j),

θ – direction of growth, which was selected randomly among 8 permissible directions shown in figure 4 (crystallographic orientation is not accounted for in the present model).

3.3. Transition rules

Transition rules define the new state of the cell in the time step $t+1$ depending on the state of this cell and the state of the neighbouring cells in the previous time step t. The general equation for the transition rules is (Szeliga & Pietrzyk, 2011):

$$Y_{i,j}^{t+1} = \begin{cases} \text{if}(\Lambda) \Rightarrow new\,state \\ \text{else} \Rightarrow Y_{i,j}^{t} \end{cases} \qquad (9)$$

where: $Y_{k,l}^{t}, Y_{k,l}^{t+1}$ – state of the cell (k,l) in the previous and current time step, respectively, Λ – logical function, which controls changes of the state of the cell.

It is seen from equation (9) that the cell can either not change its state or, if the function Λ is true, the cell changes the state to a new state. Function Λ is defined on the basis of the available knowledge about the considered process or phenomenon, which in the present paper is the bainitic transformation.

Bainite nucleates mainly at the austenite grains boundaries (γ/γ). It is due to the lower carbon content in this area. The larger is the distance from the ferrite grain, the lower is carbon concentration and the larger is probability that the cell will become a nucleus of the bainite. New nuclei of the bainite can also occur on the sheaves, which stopped to grow (Bhadeshia, 2001), but this mechanism is not accounted for in the present model. When the volume fraction of ferrite is large and austenite grain boundaries are short, the bainite can additionally nucleate inside the austenite grains. Nucleation sites for the bainite are controlled by the probability functions introduced in the transition rules.

Transition rules for nucleation are based on the above information and on the published experimental observations (Bhadeshia, 2001; Morozov et al., 2008). An assumption was made in the model that nucleation of the bainite is determined by the Gauss function of temperature:

$$P_N = \exp\left(-\frac{T_{std}}{2\sigma}\right)^2$$

where: σ – standard deviation, which in the present model is 0.25, T_{std} – temperature scaled to the [-1,1] interval:

$$T_{std} = \frac{2(B_s - T)}{B_s - M_s} - 1 \qquad (10)$$

The probability of nucleation at the austenite grain boundaries is defined as:

$$P_{N1} = P_N \frac{N_{\max}}{n_{\gamma/\gamma}} \qquad (11)$$

where: $N_{\max}$ – assumed maximum number of nuclei.

The probability of nucleation decreases when the temperature approaches B_s or M_s. It follows the idea, which is commonly used in modelling ferritic transformation, see for example (Kumar et al., 1998; Donay et al., 1996). As it was mentioned, the nucleation inside the austenite grains is also allowed in the model and the probability for this nucleation (P_{N2}) was introduced:

$$P_{N2} = P_N \frac{N_{\max} - N_{\gamma/\gamma}}{n_{\gamma}} \qquad (12)$$

In equations (11) and (12) $n_{\gamma/\gamma}$ is a number of cells located at the austenite grain boundaries and n_{γ} is a number of cells located inside the austenite grains and $N_{\gamma/\gamma}$ is a number of nuclei, which have already occurred at the austenite grain boundaries.

Taking into account mentioned above information, the following transition rule was formulated for nucleation of the bainitic ferrite:

$$Y_{i,j}^{t+1} = \begin{cases} \text{if}(\Lambda) \Rightarrow B \\ \text{else} \Rightarrow Y_{i,j}^{t} \end{cases} \qquad (13)$$

$$\Lambda = T < B_s \wedge \left[\left(Y_{i,j}^{t} = \gamma/\gamma \wedge l_{(0,1)} < P_{N1} \right) \vee \left(Y_{i,j}^{t} = \gamma \wedge P_{N1} > 1 \wedge l_{(0,1)} < P_{N2} \right) \right] \qquad (14)$$

Mobility of the interface and the diffusion of carbon are the factors, which control motion of the interface boundary. Due to decrease of the diffusion coefficient in lower temperatures, in the lower bainite the carbon is not transported to the inter lamella space and carbides precipitate in the ferrite, see lower part of figure 3.

Transition rules for growth of bainite are, to some extent, similar to those applied in modelling growth of ferrite grains during ferritic transformation. Approach proposed by Kumar et al. (1998)

is used, but ferrite is substituted by the bainitic ferrite. Velocity of the growth (v_n) is controlled by the carbon concentration gradient at the boundary:

$$v_n = D\nabla c \cdot \mathbf{n} \frac{1.0256}{c_{\gamma B}} \qquad (15)$$

where: D – diffusion coefficient, c – carbon concentration, $\mathbf{n}$ – unit vector normal to the interface, $c_{\gamma B}$ – equilibrium carbon concentration at the austenite/bainitic ferrite boundary.

Substituting the gradient by the effective distance of the diffusion and rearranging of equation (15) yields (Jabłoński, 2011):

$$v_n = \frac{1.0256\left(c_{\gamma B} - c_{\gamma}\right)}{c_{\gamma B}} \sqrt{\frac{D}{t}} \qquad (16)$$

Equation (16) describes velocity of growth of cells located in the γ/B area. Following (Lan et al., 2004) the length of the growth of the bainitic ferrite cell (i,j) inside the γ/B area is calculated as:

$$l_{i,j}^{t+1} = \int_{t}^{t+1} v_n dt \qquad (17)$$

where: t – time at which cell (i,j) changed its state into bainitic ferrite (B).

This length determines the volume fraction of bainite in the cell (i,j):

$$X_{i,j}^{t+1} = \frac{l_{i,j}^{t+1}}{L_{CA}} \qquad (18)$$

where: L_{CA} – distance between the two adjacent cells.

Taking into account mentioned above information, the following transition rule was formulated for growth of the bainitic ferrite:

$$Y_{i,j}^{t+1} = \begin{cases} \text{if}\left(\Lambda\right) \Rightarrow B \\ \text{else} \Rightarrow Y_{i,j}^{t} \end{cases} \qquad (19)$$

$$\Lambda = T < B_s \wedge \left(Y_{i,j}^{t} = \gamma / B \wedge Y_{k,l}^{t} = \right.$$
$$\left. B \wedge X_{i,j} \leq 0.5 \wedge l_{(0,1)} < P_{N3}\right) \qquad (20)$$

where: P_{N3} – probability of growth, which in the present work is assumed 0.2, k,l – indexes of the cell, which is a neighbour of the i,j cell in the direction of growth θ.

There are additional rules formulated, which control the direction of growth (Jabłoński, 2011).

These rules for the bainitic ferrite cell (i,j) are given in table 1, see figure 4 for meaning of the symbols.

Precipitation of carbides in ferrite is simulated by the model. It is assumed that carbide precipitates at minimum three cells of the ferritic bainite/austenite border, in which the carbon contents exceeds certain critical value. When cells with carbide are created, the whole excess of carbon over 0.0218% remains in these cells and the ferritic bainite/austenite boundary is moved. Each neighbour of the carbide cells changes its state into γ/B. These principles are represented by the following transition rule:

$$Y_{i,j}^{t+1} = \begin{cases} \text{if}\left(\Lambda\right) \Rightarrow \chi \\ \text{else} \Rightarrow Y_{i,j}^{t} \end{cases} \qquad (21)$$

$$\Lambda = T < B_s \wedge \left(Y_{i,j}^{t} = \gamma / B \wedge Y_{k,l}^{t} = B \wedge c_{k,l} > c_{cr}\right)$$

where: k,l – indexes of the cells, which are neighbours of the i,j cell (at least 3 cells k,l are needed to create carbide), c_{cr} – critical carbon content for creation of carbide.

4. RESULTS AND DISCUSSION

Simulations were performed for constant cooling rates and for isothermal conditions. Various cooling rates and various isothermal temperatures were applied.

4.1. Constant cooling rates

Selected results for the cooling rates of 26 K/s and 72 K/s are presented below. The CA code for ferritic transformation (Opara, 2009) is used to generate the initial microstructure for the current model of the bainitic transformation. The following information is generated by that code: boundaries of austenite grains, ferrite grains and austenite/ferrite boundaries, carbon concentration in the austenite cells. The initial microstructure for the cooling rate of 26 K/s is shown in figure 5. Volume fraction of ferrite predicted by the model was 74%. Thus, the number of cells located at the austenite grains boundaries was small and according to the transition rule (14) the model allowed nucleation of the bainitic ferrite inside the grains.

Table. 1. The rules for the selection of the growth direction.

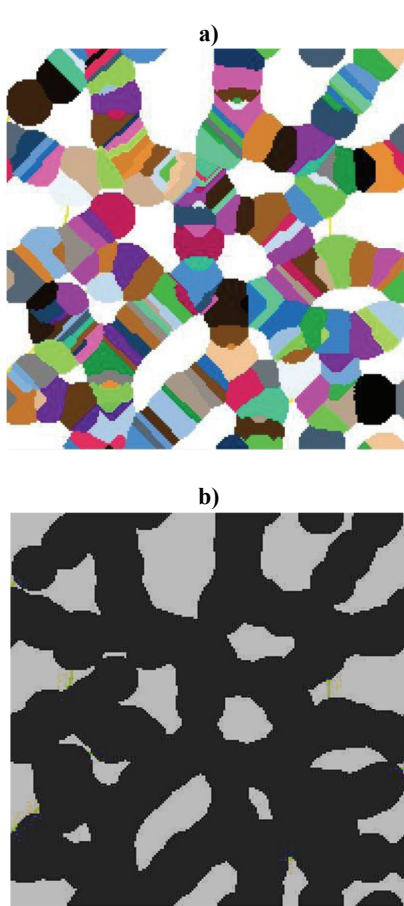| Direction	Condition
T(*i*,*j*+1)	$\Lambda = Y_{i,j-1}^{t} = B \vee \left(Y_{i-1,j-1}^{t} = B \wedge l_{(0,1)} < 0.5 \right) \cap \left(Y_{i+1,j-1}^{t} = B \wedge l_{(0,1)} \geq 0.5 \right)$
B(*i*,*j*-1)	$\Lambda = Y_{i,j+1}^{t} = B \vee \left(Y_{i-1,j+1}^{t} = B \wedge l_{(0,1)} < 0.5 \right) \vee \left(Y_{i+1,j+1}^{t} = B \wedge l_{(0,1)} \geq 0.5 \right)$
L(*i*-1,*j*)	$\Lambda = Y_{i+1,j}^{t} = B \vee \left(Y_{i+1,j+1}^{t} = B \wedge l_{(0,1)} < 0.5 \right) \vee \left(Y_{i+1,j-1}^{t} = B \wedge l_{(0,1)} \geq 0.5 \right)$
R(*i*+1,*j*)	$\Lambda = Y_{i-1,j}^{t} = B \vee \left(Y_{i-1,j+1}^{t} = B \wedge l_{(0,1)} < 0.5 \right) \vee \left(Y_{i-1,j-1}^{t} = B \wedge l_{(0,1)} \geq 0.5 \right)$
TR(*i*+1,*j*+1)	$\Lambda = Y_{i-1,j+1}^{t} = B \vee \left(Y_{i-1,j}^{t} = B \wedge l_{(0,1)} < 0.5 \right) \vee \left(Y_{i,j-1}^{t} = B \wedge l_{(0,1)} \geq 0.5 \right)$
TL(*i*-1,*j*+1)	$\Lambda = Y_{i+1,j-1}^{t} = B \vee \left(Y_{i,j-1}^{t} = B \wedge l_{(0,1)} < 0.5 \right) \vee \left(Y_{i+1,j}^{t} = B \wedge l_{(0,1)} \geq 0.5 \right)$
BR(*i*+1,*j*-1)	$\Lambda = Y_{i-1,j+1}^{t} = B \vee \left(Y_{i,j+1}^{t} = B \wedge l_{(0,1)} < 0.5 \right) \vee \left(Y_{i-1,j}^{t} = B \wedge l_{(0,1)} \geq 0.5 \right)$
BL(*i*-1,*j*-1)	$\Lambda = Y_{i+1,j+1}^{t} = B \vee \left(Y_{i,j+1}^{t} = B \wedge l_{(0,1)} < 0.5 \right) \vee \left(Y_{i+1,j}^{t} = B \wedge l_{(0,1)} \geq 0.5 \right)$

Fig. 5. Numerical microstructure generated by the CA code (Opara, 2009) for the cooling rate 26 K/s: a) microstructure with grains; b) CA space used for simulation of the bainitic presentation (gray area represents ferrite).
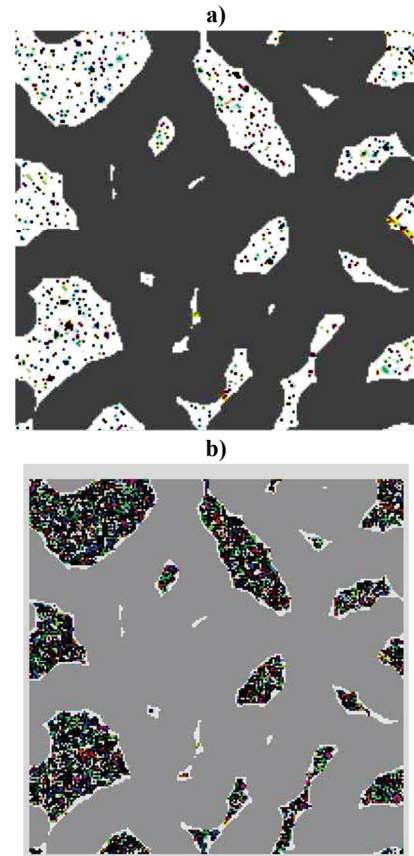

Fig. 6. Results of simulation of the bainitic transformation for the cooling rate of 26 K/s: a) after 13 CA steps; b) after completion of the transformation.

Results of simulation of the bainitic transformation for the cooling rate of 26 K/s are presented in figure 6. Figure 6a shows situation after 13 CA steps. Figure 6b shows situation when the transformation is completed. Black cells represent carbides.

Changes of volume fractions of bainite and austenite during the transformation for the cooling rate of 26 K/s are shown in figure 7. It is seen in this figure that all austenite, which remained after the ferritic transformation, was transformed into bainite.
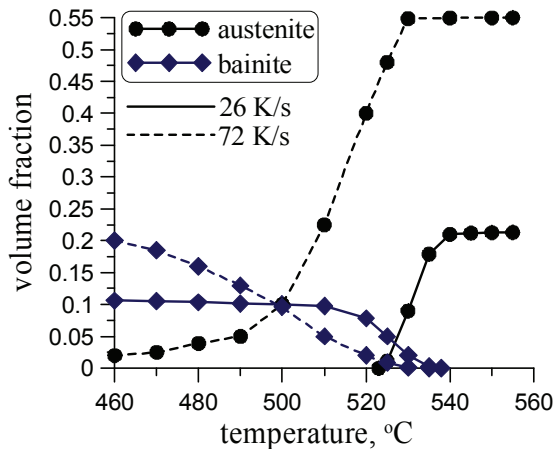
Fig. 7. *Changes of volume fractions of bainite and austenite during the bainitic transformation at the cooling rate of 26 K/s and 72 K/s.*
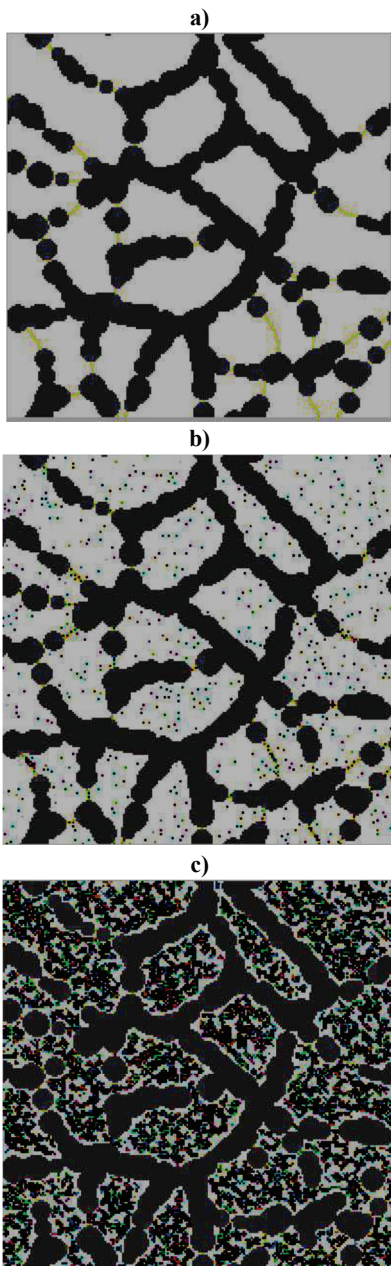
Results of simulation of the bainitic transformation for the cooling rate of 72 K/s are presented in figure 8. Figure 8a shows the initial microstructure after the ferritic transformation. The model predicted 37% of ferrite. Figure 8b shows situation after 6 CA steps. Figure 6b shows situation when the transformation is completed.

Changes of volume fractions of bainite and austenite during the transformation are shown in figure 7. It is seen in this figure that not all austenite, which remained after the ferritic transformation, was transformed into bainite. The remaining volume, which is white in figure 8c, was transformed into a martensite.
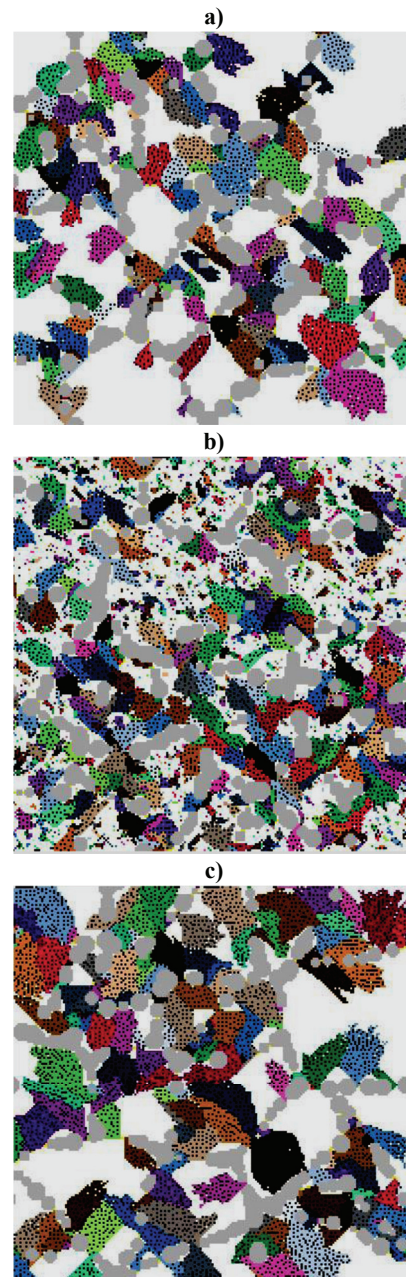
a)

b)

c)

Fig. 9. *Results of simulation of the isothermal bainitic transformation at the temperatures of 554 °C (a), 511 °C (b) and 468 °C (c).*

a)

b)

c)

Fig. 8. *Initial microstructure at the beginning of the bainitic transformation for the cooling rate of 72 K/s (a), after 6 CA steps (b) and after completion of the transformation (c).*

COMPUTER METHODS IN MATERIALS SCIENCE

4.2. Isothermal transformation

Selected results for the isothermal temperatures of 554ºC, 511ºC and 468ºC are presented below. The initial microstructure was generated by the CA code (Opara, 2009) for high cooling rate. In consequence, volume fraction of ferrite was below 10%. Results of simulations of the isothermal bainitic transformation are shown in figure 9.

Changes of volume fractions of bainite and austenite during the isothermal transformation are shown in figure 10. The effect of the temperature on the kinetics of the transformation can be observed in this figure. Among the considered temperatures, the fastest transformation was obtained for 511ºC.
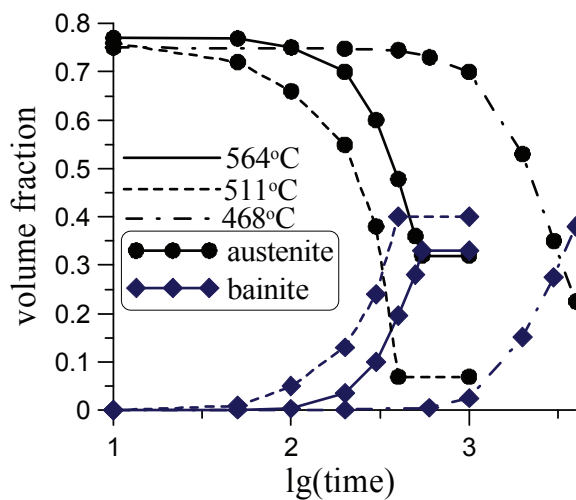

Fig. 10. Changes of volume fractions of bainite and austenite during the bainitic transformation at the isothermal temperature of 564ºC, 514 ºC and 46ºC.
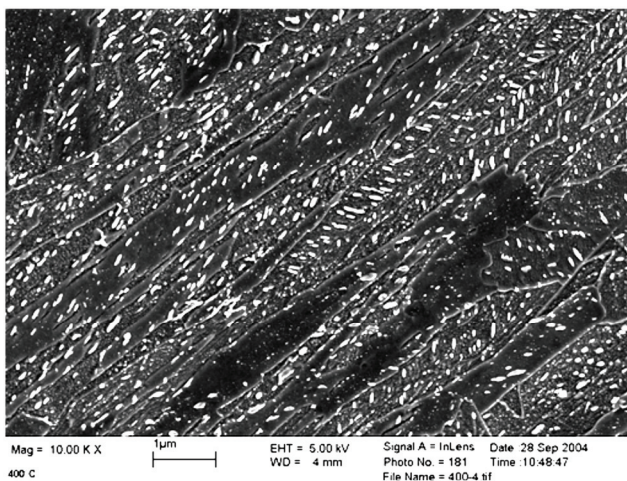

Fig. 11. Typical microstructure of the lower bainite with carbides (FEG-SEM) – courtesy of prof. Roman Kuziak.

4.3. Discussion

The presented CA model gave the results, which are in qualitative agreement with the experimental observations published in the scientific literature (Bhadeshia, 2001; Morozv et al., 2008). At some temperatures lamellar shape of the bainitic ferrite was obtained. Shape of the carbide precipitates reassembles that observed in real microstructures, see figure 11.

The effect of the temperature on the volume fraction of bainite during isothermal transformation coincides with observations made by Bhadeshia (2001). Simulation of the constant cooling rate transformation gave volume fractions of bainite similar to that obtained by Kuziak et al. (2011b) and by Sidhu et al. (2011).

Quantitative agreement of the model's predictions with experimental data at this stage is not satisfactory. It should be emphasized, however, that none of the parameters of the model was identified by fitting to the results of experiments. It is expected that identification of the model parameters, by comparison its predictions with the results of dilatometric tests, should improve the quantitative accuracy noticeably.

5. CONCLUSIONS

The predictive capabilities of the developed CA model of the bainitic transformation, which are beyond the capabilities of the existing conventional models, are as follows:

− Prediction of the nucleation of the bainitic ferrite accounting for different probability for nucleation sites located at austenite grain boundaries and inside austenite grains.
− Prediction of growth of the bainitic ferrite, accounting for the permissible directions of growth.
− Prediction of precipitation of carbides, which control growth of the bainitic ferrite.

Increase of the computing time when CA approach is coupled with the FE software and multiscale CAFE model is created is the main disadvantage. Optimization of numerical algorithms and application of parallel computing is needed to make this solution efficient.

Although the preliminary version of the CA model for the bainitic transformation is presented in the paper, the predictions of the model are qualitatively correct. Further development of the model, to improve its quantitative accuracy, should include:

− Allowing new nucleation sites of the bainite, on the sheaves, which stopped to grow.

– Accounting for the crystallographic orientations in selection of the growth directions.

– Correction to the critical carbon concentration c_{cr} in equation (21) should be introduced. Presented model assumes that maximum carbon concentration in the bainitic ferrite is 0.0218%. In real steels supersaturated ferrite can be reached in carbon, therefore, the model overestimates volume fraction of carbides.

– Identification of the coefficients in the model, by comparison its predictions with the results of dilatometric tests.

– Extending the model to upper bainite and to granular bainite.

ACKNOWLEDGEMENTS

REFERENCES

Abinandanan, T.A., Haider F., Martin G., 1998, computer simulations of diffusional phase Transformations: Monte Carlo algorithm and application to precipitation of ordered phases, *Acta Materialia*, 46, 4243-4255.

Bhadeshia, H.K.D.H., 2001, *Bainite in steels,* University Press, Cambridge.

Bhadeshia, H.K.D.H., Edmonds, D.V., 1980, The mechanism of bainite formation in steels, *Acta Metallurgica*, 28, 1265-1273.

Christian, J.W., 1975, *The theory of transformation in metals and alloys*, Pergamon Press, Oxford.

Donnay, B., Herman, J.C., Leroy, V., Lotter, U., Grossterlinden, R., Pircher, H., 1996, Microstructure Evolution of C-Mn Steels in the Hot Deformation Process: The STRIPCAM Model, *Proc. 2nd Conf. Modelling of Metal Rolling Processes*, eds, Beynon, J.H., Ingham, P., Teichert, H., Waterson, K., London, 23-35.

Hofmann, H., Mattissen, D., Schaumann, T.W., 2009, Advanced Cold Rolled Steels for Automotive Applications, *Steel Research International*, 80, 1, 22-28.

Honeycombe, R.W.K., Pickering, F.B., 1972, Ferrite and bainite in alloy steels, *Metallurgical and Materials Transactions B*, 3, 1099-1112.

Jabłoński G., 2011, *Zastosowanie metody automatów komórkowych do modelowania przemian fazowych w stalach bainitycznych*, MSc thesis, AGH, Kraków (in Polish).

Kooi, B.J., 2004, Monte Carlo simulations of phase transformations caused by nucleation and subsequent, *Physical Review B*, 70, 224108/1-12.

Kumar, M., Sasikumar, R., Kesavannair, P., 1998, Competition between nucleation and growth of ferrite from austenite - studies using cellular automaton simulations, *Acta Materialia*, 46, 6291-6303.

Kundu, S., Dutta, M., Ganguly, S., Chandra, T., 2004, Prediction of phase transformation and microstructure in steel using cellular automaton technique, *Scripta Materialia*, 50, 891-895.

Kuziak, R., Skóra, M., Węglarczyk, S., Paćko, M., Pietrzyk, M., 2011a, Computer aided design of the manufacturing chain for fasteners, *Computer Methods in Materials Science*, 11, 243-250.

Kuziak, R., Pidvysots'kyy, V., Węglarczyk, S., Pietrzyk, M., 2011b, Bainitic steels as alternative for conventional carbon-manganese steels in manufacturing of fasteners - simulation of production chain, *Computer Methods in Materials Science*, 11, 443-462.

Lan, Y.J., Li, D.Z., Li, Y.Y., 2004, Modeling austenite decomposition into ferrite at different cooling rate in low-carbon steel with cellular automaton method, *Acta Materialia*, 52, 1721-1729.

Luzginova, N.V., Zhaoa, L., Sietsma, J., 2008, Bainite formation kinetics in high carbon alloyed steel, *Materials Science and Engineering A*, 481-482 A, 766-769.

Mahnken, R., Schneidt, A., Tschumak, S., Maier, H.J., 2011, On the simulation of austenite to bainite phase transformation, *Computational Materials Science*, 50, 1823-1829.

Militzer, M., 2011, Phase field modeling of microstructure evolution in steels, *Current Opinion in Solid State and Materials Science*, 15, 106-115.

Morozov, Y.D., Matrosov, M.Y., Nastich,S.Y., Arabei, A.B., 2008, New generation of high-strength tube steels with a ferrite-bainite structure, *Metallurgist*, 52, 450-456.

Opara, J., 2009, *Ocena możliwości zastosowania automatów komórkowych do modelowania przemiany austenit-ferryt*, MSc thesis, AGH, Kraków (in Polish).

Pernach, M., Pietrzyk, M., 2008, Numerical solution of the diffusion equation with moving boundary applied to modeling of the austenite-ferrite phase transformation, *Computational Materials Science*, 44, 783-791.

Pernach, M., Pietrzyk, M., 2011, Wyznaczanie twardości martenzytu w stalach dp poprzez rozwiązanie równania dyfuzji z ruchomą granicą, *Proc. 2nd Kongres Mechaniki Polskiej*, Poznań, (in Polish), (CD ROM).

Pietrzyk, M., Madej, Ł., Rauch, Ł., Gołąb, R., 2010, Multiscale modelling of microstructure evolution during laminar cooling of hot rolled DP steel, *Archives of Civil and Mechanical Engineering*, 10, 57-67.

Scheil, E., 1935, Anlaufzeit der Austenitumwandlung, *Arch. Eissenhuttenwesen*, 12, 565-67.

Sidhu, G., Bhole, S.D., Chena, D.L., Essadiqi, E., 2011, An improved model for bainite formation at isothermal temperatures, *Scripta Materialia*, 64, 73-76.

Suehiro, M., Senuma, T., Yada, H., Sato, K., 1992, Application of mathematical model for predicting microstructural evolution to high carbon steels, 32, *ISIJ International*, 433-439.

Szeliga, D., Pietrzyk, M., 2011, Multiscale models and metamodels in application to metal forming simulations, *Proc. MEFORM 2011*, Freiberg, 364-369.

van Bohemena, S.M.C., Sietsma, J., 2010, The kinetics of bainite and martensite formation in steels during cooling, *Materials Science and Engineering A*, 527A, 6672-6676.

Waengler, S., Kawalla, R., Kuziak, R., 2008, High strength–high toughness bainitic steels alloyed with niobium for long products, *steel research international*, 79, spec. ed. Metal Forming Conf., 2, 273-279.

Zajac, S., Schwinn, V., Tacke, K.H., 2005, Characterization and quantification of complex bainitic microstructures in high and ultra-high strength linepipe steels, *Materials Science Forum*, 500-501, 387-394.

Zhang, L., Zhang, C.B., Wang, Y.M., Wang, S.Q., Ye, H.Q., 2003, A cellular automaton investigation of the transformation from austenite to ferrite during continuous cooling, *Acta Materialia*, 51, 5519-5527.

ZASTOSOWANIE AUTOMATÓW KOMÓRKOWYCH DO MODELOWANIA PRZEMIANY BAINITYCZNEJ W STALACH

Streszczenie

W pracy przedstawiono model przemiany bainitycznej w stalach wykorzystujący metodę automatów komórkowych. Dyskretny charakter tej metody pozwolił na odtworzenie węglików w ferrycie bainitycznym. Przeprowadzone testy numeryczne wykazały, że model opisują jakościowo poprawnie zjawiska zachodzące podczas przemiany bainitycznej. Wprawdzie dokładność jakościowa modelu nie jest satysfakcjonująca, to jednak możliwości obliczeniowe tego modelu są znacznie szersze w porównaniu ze stosowanymi obecnie modelami konwencjonalnymi. Można oczekiwać, że dalsze badania w kierunku identyfikacji parametrów modelu powinny poprawić w sposób znaczący jego dokładność ilościową.